Observation of Incoherent Diffraction Radiation from a Single-Edge Target in the Visible-Light Region

T. Muto,[1] S. Araki,[2] R. Hamatsu,[1,*] H. Hayano,[2] T. Hirose,[1] P. Karataev,[1] G. Naumenko,[3] A. Potylitsyn,[3] and J. Urakawa[2]

[1]*Tokyo Metropolitan University, 1-1 Minamiohsawa, Hachioji, Tokyo 192-0397, Japan*
[2]*KEK:High Energy Accelerator Research Organization, 1-1 Oho, Tukuba, Ibaraki 300-0801, Japan*
[3]*Tomsk Polytechnic University, 634050, pr.Lenina 2a, Tomsk, Russia*

(Received 21 October 2002; published 14 March 2003)

An experiment to investigate the diffraction radiation from a single edge target has been performed at the accelerator test facility of KEK with the aim of developing noninvasive beam diagnostics. The yield and the angular distribution of diffraction radiation as a function of the impact parameter was measured in the visible light region. The distributions were qualitatively consistent with the theoretical expectation. This work exhibits the first observation of the incoherent diffraction radiation in the visible light region.

DOI: 10.1103/PhysRevLett.90.104801 PACS numbers: 41.60.–m, 41.75.Ht

Extremely low emittance and high current electron beam are the vital characteristics for linear colliders and x-ray free electron lasers (FEL's). Parallel developments of noninvasive beam diagnostics are strongly required for realizing such beams. Detection of diffraction radiation in the visible wavelength region, called the optical diffraction radiation (ODR), because of its nondestructive nature, is the most promising technique for application to noninvasive beam diagnostics. A new nonperturbing beam diagnostics was proposed in [1], based on the measurement of the angular distribution of the ODR emitted by the beam when crossing a slit in a metallic foil. However, very few experimental investigations existed: measurements of the longitudinal bunch profile of an electron beam using a coherent diffraction radiation in millimeter and submillimeter wavelength regions [2–5] and the observation of the ODR with optical transition radiation (OTR) backgrounds because of a large beam size [6].

A series of experiments on ODR using an extremely low emittance electron beam extracted from the damping ring of the KEK-ATF (Accelerator Test Facility for Linear Colliders) [7,8] has been performed. The bunch length of the electron beam was 9 mm (= 30 ps) [9]; therefore, the diffraction radiation was incoherent in the wavelength region ($\lambda < 1$ μm). Experiments aimed at investigating general characteristics of the ODR and establishing a scheme of measurement for applications to a new noninvasive beam diagnostics. As a first stage of experiments the ODR from a single edge target was measured.

ODR is emitted when a charged particle passes through a vicinity of a conducting target with the impact parameter h, which satisfies a condition

$$h \leq \frac{\gamma\lambda}{2\pi}, \tag{1}$$

where γ is the Lorentz factor and λ is the ODR wavelength. There are two radiation directions. One is along the direction of particle velocity (forward radiation), the other is along the direction of specular reflection (backward radiation). When a particle passes through the vicinity of a semi-infinite plane at 45° incident angle, the backward radiation is emitted at 90° from the particle trajectory. In the case of the relativistic electron, the angular distribution of ODR is given by [10–12]

$$\frac{d^2W}{d\omega d\Omega} = \frac{\alpha}{4\pi^2}\exp\left(-\frac{\omega}{\omega_c}\sqrt{1+\gamma^2\theta_x^2}\right) \times \frac{\gamma^{-2}+2\theta_x^2}{(\gamma^{-2}+\theta_x^2)(\gamma^{-2}+\theta_x^2+\theta_y^2)}, \tag{2}$$

where α is the fine-structure constant, the characteristic photon energy $\omega_c = \gamma/2h$ (we used the system of units $\hbar = m = c = 1$), and the observation angles θ_x and θ_y are depicted in Fig. 1.

On the other hand, OTR is emitted when a charged particle crosses the boundary between two media with

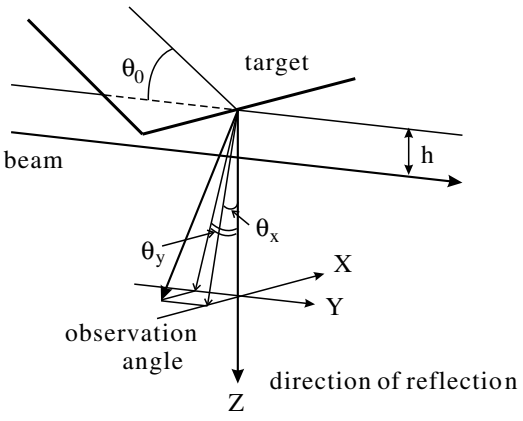

FIG. 1. Geometry of DR near a semi-infinite target.

different dielectric constants. OTR will be emitted in the forward and the backward directions as well as the ODR. In relativistic electron case, the angular distribution of OTR for an infinite boundary surface is given by [13]

$$\frac{d^2W}{d\omega d\Omega} = \frac{\alpha}{\pi^2}\frac{\theta^2}{(\gamma^{-2}+\theta^2)^2}, \tag{3}$$

where $\theta^2 = \theta_x^2 + \theta_y^2$ is the angle between the observation direction and the direction of specular reflection. As seen in Eq. (3), the distribution has a maximum at $\theta_{max} = 1/\gamma$ and is symmetric in the azimuthal direction around the radiation axis. Comparing Eqs. (2) and (3) one can see an explicit wavelength dependence of the ODR intensity [via the $\exp(-\omega/\omega_c)$ term] in contrary to the OTR.

An ODR and OTR measurement system has been constructed at the extraction line of KEK-ATF, which provides a 1.28 GeV ($\gamma \sim 2500$) single bunch electron beam extracted from the damping ring. The experimental setup is shown in Fig. 2. The measurement system is composed of an alignment laser system, screen monitors, a target chamber, aluminum coated plane mirrors, a slit, a photomultiplier tube (PMT), and a Cherenkov counter for detecting γ rays.

A target holder is mounted at 45° with respect to the beam line in the target chamber and actuated by a pulse motor stage. The target position can be read by a linear gauge with a precision of 0.5 μm. The target is 0.5 μm thick aluminum coated on a silicon wafer 300 μm thick. Roughness of the target surface is less than Ra = 0.15 μm.

Lights from the target surface (backward OTR, ODR, and other backgrounds) were directed downward from the beam line to a mirror rotatable with respect to horizontal and vertical axes. Angles of the mirror are rotated by micromotor head actuators remotely controlled by a computer with a precision of 54 μrad and 29 μrad horizontally and vertically, respectively. As the rotatable mirror and the light detector are placed at the distances of 0.92 m and 2.60 m, respectively, from the target, the maximum resolutions for the angular distribution measurements were 35 μrad and 19 μrad in θ_x and θ_y, respectively. PMT (Hamamatsu H1161) is used as a light detector. The range of the spectral response of the PMT is from 300 to 650 nm. A slit of which the horizontal and vertical widths can be adjusted independently is located in front of the PMT.

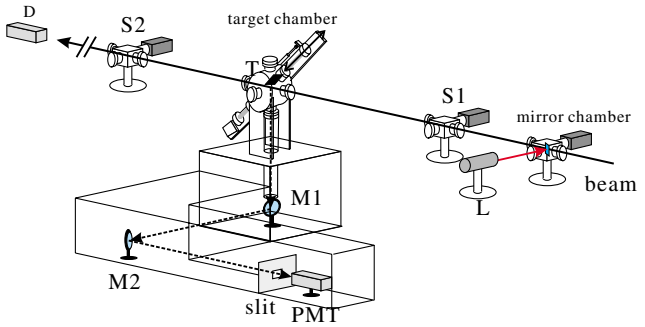

FIG. 2 (color online). Experimental setup. T: target; L: alignment laser; S1,S2: screen monitors; M1: rotatable mirror; M2: fixed mirror; D: Cherenkov counter.

The measurement system was aligned by an optical system composed of a He-Ne laser, a spatial filter, and a focusing lens ($f = 100$ mm). These components are mounted on a single optical base, of which position and direction each can be adjusted horizontally and vertically by micrometers and adjustable screws. The optical alignment was performed in the following manner. The beam positions at the two screen monitors were recorded by capturing the beam profile images in advance. In order to determine the beam axis on the target, a focused laser light was introduced into the beam line along the beam trajectory from the upstream mirror chamber. Laser light positions on the screens were adjusted to coincide with the recorded beam positions by the optical alignment system. Throughout the experiment the laser beam position was adjusted within 100 μm accuracy at both screens. Since the distance between two screen monitors was 4.8 m, the alignment of the optical system was adjusted within 42 μrad.

The beam was operated in a single bunch mode, at 1.28 GeV energy, with 1.56 Hz repetition and with the intensity of 7×10^9 electrons per bunch. The beam size at the target was estimated to be $\sim$80 μm horizontally and $\sim$8 μm vertically. Horizontal and vertical widths of the slit in front of the PMT were set at 500 μm.

The impact parameter h is the key parameter for the ODR measurement. In order to determine the target edge position, the intensity of the γ ray produced through the Bremsstrahlung at the target was measured as a function of the target position. The result is shown in Fig. 3.

If the target was a perfect plate and the electron beam was a Gaussian in profile, the γ ray intensity can be calculated analytically,

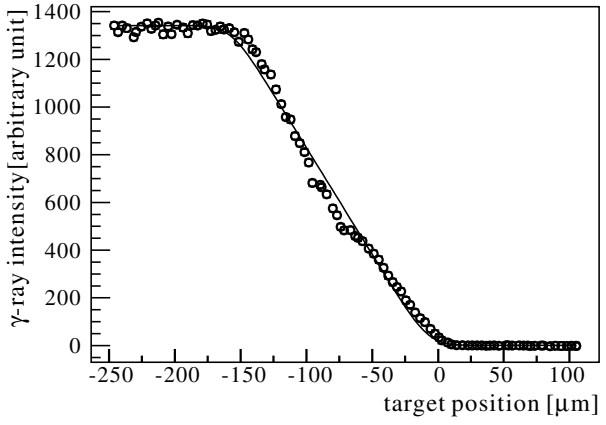

FIG. 3. The γ ray intensity as a function of the target position (open circles). The γ ray intensity was corrected by the beam intensity. The solid curve is the result of the fit to Eq. (4). See text.

$$I(x) = I_{\max} \times \left[\frac{\sigma^2}{2t\cos\theta}\left(e^{-(x^2/2\sigma^2)} - e^{-(x-t\cos\theta)^2/2\sigma^2}\right) + \sqrt{\frac{\pi}{2}}\frac{\sigma}{2t\cos\theta}\left\{(x - t\cos\theta) \times \mathrm{erf}\left(-\frac{x - t\cos\theta}{\sqrt{2\sigma^2}}\right) - x \times \mathrm{erf}\left(-\frac{x}{\sqrt{2\sigma^2}}\right) + t\cos\theta\right\}\right], \quad (4)$$

where x is the beam position, $I_{\max}$ is the maximum intensity, t is the target thickness, θ is the target angle with respect to the beam line, σ is the rms size of the beam, and erf is the error function. The vertical beam size is much smaller than the target thickness, so the electron path length through the material, and hence the γ ray intensity, should show a variation of inclined target thickness when the target is moved to the beam orbit. The intensity as a function of the target position was expected to be close to linear; however, a little dent is seen in the middle of the slope. We considered that there was a rough part in the target edge. To determine the target edge position, four parameter ($I_{\max}$, t, σ and the target edge position) fitting to Eq. (4) was performed using all data points and the result is shown by a solid curve in Fig. 3. Independent fittings were performed by excluding data points in the middle part and slightly different edge positions were obtained. We estimated the maximum error on the determination of the target edge position to be 11 μm by taking the difference between fitted edge positions.

For the evaluation of the performance of the measurement system, the angular distribution of the OTR was measured and compared with the theoretical distribution. A typical angular distribution with respect to θ_x is shown in Fig. 4. The measured opening angle between two maxima was close to the theoretical one ($= 2/\gamma$). The same opening angle in θ_y was also observed (not shown). The detection system was confirmed to function well for the angular measurements. On the other hand, as seen in Fig. 4 there is an asymmetry of 22% in the height of peaks, while less asymmetry (7%) was observed in θ_y (not shown). These were considered to be coming from a possible surface deformation of the target or from background lights reflected by the surface of the target.

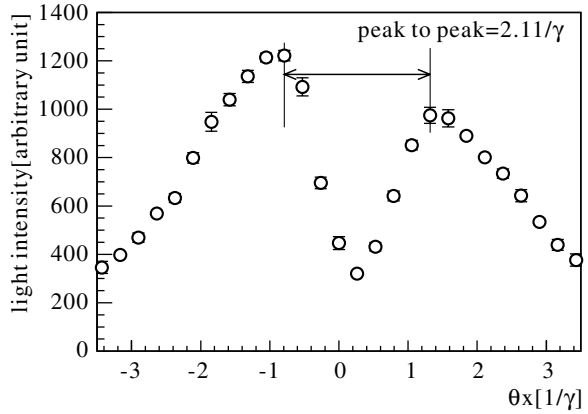

FIG. 4. Transition radiation angular distribution ($\theta_y = 0$).

Then, we measured the light yield as a function of the impact parameter at the fixed mirror position ($\theta_x = \theta_y = 0$). The result is shown in Fig. 5, where the normalization was performed relative to the maximum of the OTR intensity.

We observed the light yield at the impact parameter where no Bremsstrahlung γ ray was detected. This means that the light was emitted when the electron beam did not hit the target. In order to confirm the light signal was really coming from the target, we masked the PMT then no signal was detected.

There were backgrounds from the synchrotron radiation coming from the bending magnets. The contribution of the backgrounds to the OTR light yield was estimated to be at most 22% from the asymmetry of the angular distributions. Since the observed light yield shown in Fig. 5 was comparable to the OTR, we estimated that the contribution of the background to the light yield at the target edge was the same level as the OTR.

We made a comparison between experimental results and the theoretical calculations based on the model [12] that allows one to calculate both ODR and OTR yields taking into account the edge effect on the latter one. The uniform sensitivity of the PMT in the above mentioned wavelength range and the finite angular aperture of the detector were included in the calculation. As seen in Fig. 5, the calculation reproduces quite well the impact parameter dependence of the light yield, in particular, at the target edge where the measured light intensity agrees with the OTR maximum yield as the model predicted and also in the wide impact parameter range covering both the OTR and the ODR.

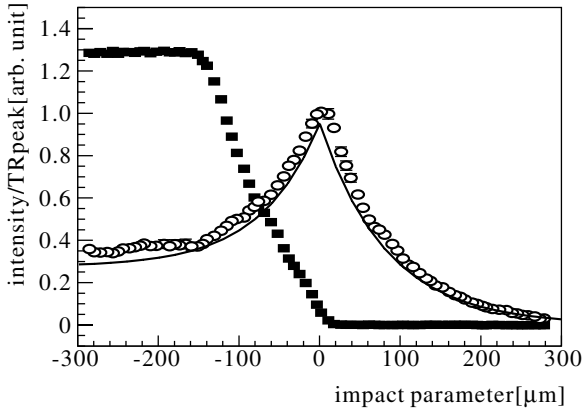

FIG. 5. Impact parameter dependence of intensities. Black squares: the γ ray intensity; open circles: the relative light yield; solid curve: calculated.

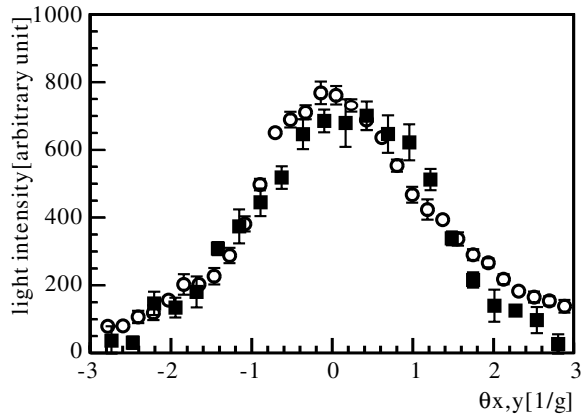

FIG. 6. DR angular distributions at $h = 41$ μm. Open circles are θ_y distribution at $\theta_x = 0$; black squares are θ_x at $\theta_y = 0$.

We have measured angular distributions of the ODR at different impact parameters. A typical example of angular distributions for θ_x and θ_y at $h = 41$ μm is shown in Fig. 6. FWHM widths of angular distributions as a function of the impact parameter are plotted in Fig. 7; also shown in the figure are curves calculated from Eq. (2). Although there are differences between the experimental results and the theoretical calculation, results are consistent with the expectations of the incoherent visible light of the ODR, when taking into account the fact that the backgrounds were not eliminated completely.

In summary, we have performed a series of ODR experiments. The prime purpose is to investigate the ODR from a single edge target. We measured the intensity of the light from the target as a function of the impact parameter. We confirmed the light yields at the impact parameter where the beam did not hit the target. The impact parameter dependence of the light yield was consistent with the theoretical calculations taking into account both the OTR and ODR. From these considerations we concluded that we have observed the incoherent diffraction radiation in the visible wavelength region at the first time. Since present experiments on the ODR from a single edge target showed good agreement with theoretical calculations based on the same principle as in [1], the measurement of the ODR from the slit target will be a promising technique for noninvasive and instantaneous beam diagnostics.

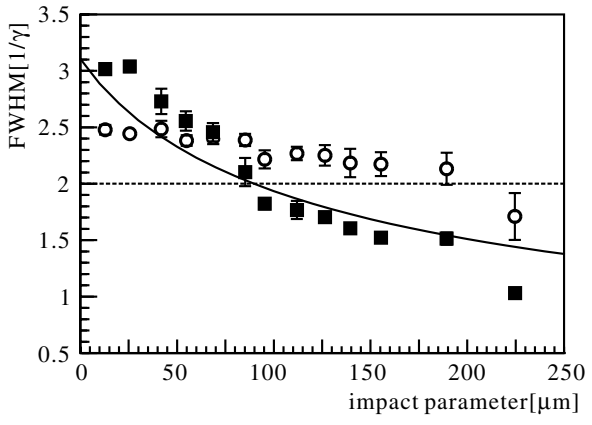

FIG. 7. FWHM of the ODR angular distribution as a function of the impact parameter: circles: θ_x (experiment); squares: θ_y (experiment); dashed curve: θ_x (calculation); solid curve: θ_y (calculation).

We thank all members of the KEK-ATF group for technical support and beam operation during this experiment. The authors thank Professor H. Sugawara, Professor Y. Kamiya, and Professor A. Enomoto of KEK for their continuous support and encouragement. One of the authors (A. P.) acknowledges the Advanced Compact Accelerator Project of National Institute of Radiological Sciences for the financial support.

*Corresponding author.
Electronic address: hamatsu@phys.metro-u.ac.jp

[1] M. Castellano, Nucl. Instrum. Methods Phys. Res., Sect. A **394**, 275 (1997).
[2] Y. Shibata, S. Hasebe, K. Ishi, T. Takahashi, T. Ohsaka, M. Ikezawa, T. Nakazato, M. Oyamada, S. Urasawa, T. Yamakawa, and Y. Kondo, Phys. Rev. E **52**, 6787 (1995).
[3] M. Castellano, V. A. Verzilov, L. Catani, A. Cianchi, G. Orlandi, and M. Geitz, Phys. Rev. E **63**, 056501 (2001).
[4] A. H. Lumpkin, N. S. Sereno, and D.W. Rule, Nucl. Instrum. Methods Phys. Res., Sect. A **475**, 470 (2001).
[5] B. Feng *et al.*, Nucl. Instrum. Methods Phys. Res., Sect. A **475**, 492 (2001).
[6] I. E. Vnukov, B. N. Kalinin, G. A. Naumenko, D.V. Padalko, A. P. Potylitsyn, and O.V. Chefonov, JETP Lett. **67**, 802 (1998).
[7] J. Urakawa, H. Hayano, K. Kubo, S. Kuroda, N. Terunuma, M. Kuriki, T. Okugi, T. Naito, S. Araki, A. Potylitsyn, G. Naumenko, P. Karataev, N. Potylitsyna, I. Vnukov, T. Hirose, R. Hamatsu, T. Muto, M. Ikezawa, and Y. Shibata, Nucl. Instrum. Methods Phys. Res., Sect. A **472**, 309 (2001)
[8] ATF Collaboration, K. Kubo *et al.*, Phys. Rev. Lett. **88**, 194801 (2002).
[9] K. L. F. Bane, T. Naito, T. Okugi, Q. Qin, and J. Urakawa, SLAC Report No. SLAC-PUB-8846, 2001.
[10] A. P. Kazantsev and G. I. Surdutovich, Sov. Phys. Dokl. **7**, 990 (1963).
[11] M. L. Ter-Mikaelyan, *High Energy Electromagnetic Processes in Condensed Media* (Wiley/Insterscience, New York, 1972).
[12] A. P. Potylitsyn, Nucl. Instrum. Methods Phys. Res., Sect. B **145**, 169 (1998).
[13] L. Wartski, S. Roland, J. Lasalle, and M. Bolore, J. Appl. Phys. **46**, 3644 (1975).